

ON THE APPROACH TO STABILITY OF PULSAR AVERAGE PROFILES

N. RATHNASREE AND JOANNA M. RANKIN

Raman Research Institute, Bangalore 560080, India

Received 1995 January 10; accepted 1995 April 28

ABSTRACT

We have studied the rate of stabilization to a global average profile for over two dozen radio pulsars. To investigate the physical processes governing the approach to a stable profile, the pulse-to-pulse profile variations have been separated into three components: variations arising from the changes in the intensity, phase, and width of the pulse maximum. The rate of stabilization is seen to vary from pulsar to pulsar, and a correlation analysis of this rate with other pulsar properties gives some insight into the processes governing irregular variations from pulse to pulse. The stabilization rate for the polarized emission has also been studied, and it is seen that this rate generally is slower than the stabilization rate for the total intensity. In many cases there is a sharp change in the stabilization rate after approximately 4–100 pulses are averaged.

Subject heading: pulsars: general

1. INTRODUCTION

Pulsed radio emission from pulsars shows variability over several timescales. In contrast, pulsar profiles integrated over several hundred pulses are remarkably stable, except for the phenomena of nulling and mode changing that occurs in some pulsars. Helfand, Manchester, & Taylor (1975, hereafter HMT75) studied the approach to stability for about one-half dozen pulsars. They concluded that there exists a characteristic timescale for each pulsar over which a stable pulse profile is obtained. This timescale is different from pulsar to pulsar and seems to be correlated with other pulsar properties. For instance, HMT75 find that pulsars which show drifting sub-pulses stabilize faster than those which do not show any noticeable drifting behavior. There exists no systematic study of the timescale over which pulsar profiles stabilize for any sample of pulsars other than the study of HMT75.

We have investigated the formation times for a stable pulse profile for ≈ 28 pulsars, some of which were also included in the sample of HMT75. Remarkably, we obtain very nearly the same results as HMT75 for these pulsars. This suggests that the stabilization rates for profile formation are very stable over these timescales. The timescales over which single pulses are averaged out to give a stable profile differ characteristically from pulsar to pulsar. This seems to suggest that the processes which perturb a stable emission profile do not consist purely of noise.

2. STABLE PROFILE FORMATION

Observations were carried out in a single observing session during 1992 October at Arecibo. The observations were principally at frequencies of 430 and 1414 MHz. Stokes parameters were calculated pulse by pulse for some 100–500 phase bins in selected windows of pulse longitude. One window covered a longitude region with no emission, and other windows were chosen to cover the various components of the pulsed emission (main pulse, interpulse, etc). The average intensity in the noise window was then subtracted from the total intensity at each phase bin to determine the baseline-subtracted total intensity. Sequences of several hundred pulses were obtained for each

pulsar mostly at 1414 MHz and for a few pulsars at 430 MHz. A global average profile was obtained for each pulsar by synchronously averaging all the pulses.

To determine a measure of the rate at which the profile stabilizes when subaverages are obtained over smaller numbers of periods than those included in the global average profile, the procedure of HMT75 was adopted. Sets of subaveraged profiles were obtained over $n = 2^m$ adjacent pulses, in which $m = 0, 1$ such that 2^l is less than one-half the total number of periods. This is to ensure that at least two independent subaverages are obtained in every case. The intensity distribution for each of the subaveraged profiles was then scaled in such a way that the integrated intensity for the subaveraged profile was equal to that for the global average profile. As in HMT75, the correlations of these subaveraged profiles with the global profile are used to define the rate of stabilization of subaveraged profiles.

Cross-correlation coefficients X_n^k for intensity distributions between the subaveraged profile and the global profile were obtained for each subaverage of 2^m periods. For each value of n , k independent subaverages are formed, where $k = \text{integer}(N/2^m)$, where N is the total number of pulses observed. The average cross-correlation coefficient X_n for subaverages of 2^m periods was then obtained by averaging over all the k independent subaverages. The procedure followed by HMT75 was to delete the cross-correlations obtained from those subaverages whose total intensity was less than 10% of the intensity of the global average profile. However, since some of the pulsars included in our study have distinct nulls and the intrinsic stabilization rate for a pulsar also depends on the frequency and duration of nulls, we think it judicious to include all the subaverages while calculating the average cross-correlations. However, in order to facilitate comparisons of our results with those of HMT75, averaged cross-correlations with the low-intensity subaverages removed were also calculated.

The behavior of $(1 - X_n)$ with n gives a measure of the rate of stabilization. In general, this function exhibits a power-law behavior, with some pulsars also having a change in the power-law index occurring at some intermediate periods. Figure 1 shows the behavior of $\log(1 - X_n)$ with $\log(n)$ for some of the pulsars included in this study. (These figures also show the variation of $[1 - X_n]$ for the profiles of linearly polarized flux.

¹ On leave from the University of Vermont.

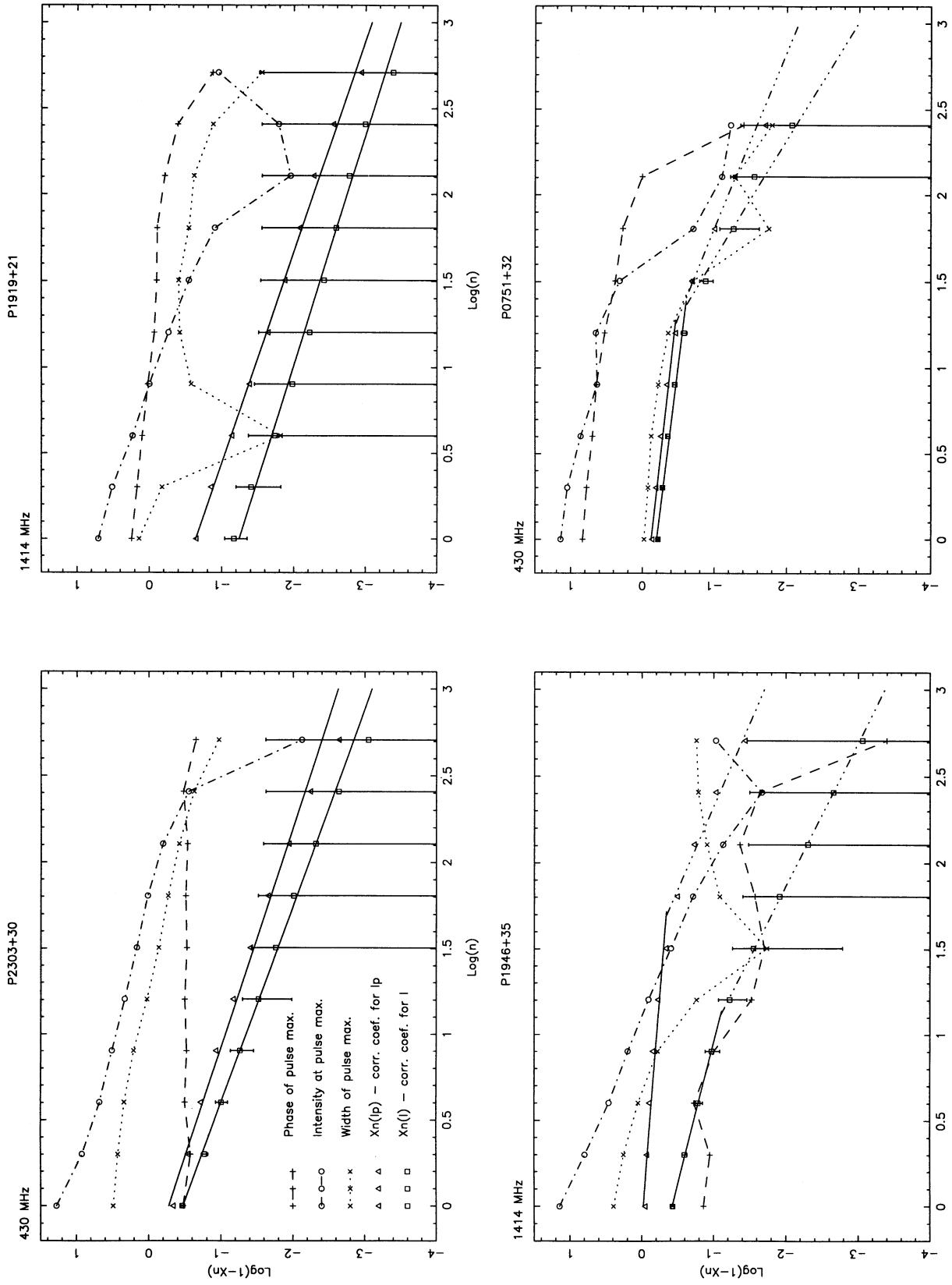


FIG. 1.—The variations of $\log(1 - X_p)$ (correlation coefficient X_p of subaverages with the global average profile) with $\log(n)$ (number of periods included in the subaverage) are shown for some of the pulsars studied. The error bars shown are the rms values for a given n . The data fitted with straight lines show the variations for the total power $[X_n(l)]$ and the polarized power $[X_n(l_p)]$. Also shown are the variations in the differences of the phase, intensity, and width of the pulse maximum for the subaverages with the corresponding quantity for the global average profile.

In addition, the differences in the values of the intensity at the pulse maximum, its width and the phase at maximum between the subaveraged profiles, and the global profile are also shown in these figures for comparison.) A single slope describes the variation of $\log(1 - X_n)$ with $\log(n)$ in the case of only a few pulsars. For the majority of the pulsars a distinct break is seen. Three quantities in such figures seem to reflect the stabilization behavior: (1) the single-pulse correlation coefficient, (2) the slopes of the $\log(1 - X_n) - \log(n)$ line, and (3) the existence and the location of a break in the slope. PSR 1919+21 has the highest single-pulse correlation coefficient among the pulsars shown in Figure 1. Single-pulse sequences (not shown) of this pulsar have a structure very similar to the average profile, accounting for its high single-pulse correlation coefficient. In general, the structure, i.e., the number of components and their relative heights, in the average profile has contributions both from the structure in the single pulses as well as the frequency of occurrence of the pulse maximum at different phases of the pulse. Single pulses from PSR 0751+32 mostly do not have the double-peaked structure shown in the average profile. The frequency of occurrence of the pulse peak is high inside the two peaks seen in the average profile, thus accounting for the different structure seen in the average profile from the single pulses.

This explains the low single-pulse correlation coefficient seen in this pulsar.

Generally, the stabilization rate in pulsars with high single-pulse correlation coefficients, like PSR 1919+21 or PSR 1929+10, is described by a single power-law index. In contrast, pulsars with nulling or moding such as PSR 0751+32 or PSR 1944+17 have very low values of the single-pulse correlation coefficient and distinct breaks in the power-law index describing the stabilization rate. A number of pulsars have moderate values of the single-pulse correlation coefficient and also distinct breaks in the slope (PSR 1946+35, in Fig. 1). Breaks in the slope of the correlation coefficient curves were also seen in the case of some pulsars in the sample of HMT75. This was attributed by HMT75 to the existence of a correlated activity at those timescales in which a break in the slope occurs. They concluded that pulsars showing drifting subpulse behavior have breaks in the slope between 4–16 periods, while pulsars which show mode-changing or nulling phenomena have breaks in the slope around 100 periods. This behavior is confirmed in our larger sample, although the breaks occur over a somewhat wider range of periods. This can be seen from the results shown in Table 1. This table lists all the pulsars for which stability analysis was done, the approximate pulse

TABLE 1
PROFILE STABILIZATION PARAMETERS

Pulsar (1)	P (s) (2)	\dot{P}_{-15} (3)	Pulses (4)	S/N (5)	n_t (6)	s_t^1 (7)	s_t^2 (8)	n_{I_p} (9)	$s_{I_p}^1$ (10)	$s_{I_p}^2$ (11)	α (12)	ρ (13)	Type (14)
0301+19l	1.387	1.296	734	3.5, ...	62	-0.31	-1.88	32	-0.20	-0.58	30.0	3.7	D
0540+23l	0.245	15.428	3023	10.4, ...	9	-0.49	-1.01	11	-0.38	-1.03	38.0	...	S_t
0611+22u	0.334	59.630	1224	3.37, ...	6	-0.50	-1.05	12	-0.38	-0.91	36.0	...	S_t
0611+22l	6000	4.2, ...	0	-0.67	-0.67	4	-0.45	-0.69
0626+24l	0.476	1.990	2500	5.0, ...	13	-0.84	-1.06	17	-0.84	-1.12	30.0	...	S_t
0751+32u	1.442	1.074	1063	15.6, ...	23	-0.29	-1.45	18	-0.26	-0.98	26.0	4.8	D
0820+02u	0.864	0.103	1142	10.9, 10.8	5	-0.64	-0.80	4	-0.46	-0.79	46.0	4.8	S_d
0820+02l	1561	2.3, ...	5	-0.56	-0.77	22	-0.17	-0.59
0823+26u	0.530	1.723	1800	107.6, 44.9	0	-0.90	-0.90	0	-0.87	-0.87	84.0	8.2	S_t
0823+26l	4080	40.8, 19.7	21	-0.81	-1.11	16	-0.68	-1.09	S_t
0943+10u	1.097	3.529	986	15.7, 14.7	13	-0.46	-0.73	10	-0.34	-0.66	11.5	5.6	S_d
1133+16u	1.187	3.732	956	...	28	-0.73	-1.19	24	-0.64	-1.03	46.0	5.3	D
1133+16l	2188	112.2, 14.7	23	-0.71	-1.05	23	-0.59	-1.07
1821+05l	0.752	0.225	2564	8.3, 7.0	11	-0.73	-1.03	14	-0.44	-1.00	32.0	7.0	T
1839+09l	0.381	1.091	1128	3.8, ...	15	-0.68	-1.12	44	-0.28	-0.98	83.0	6.6	T
1842+14l	0.375	1.866	1091	3.2, ...	11	-0.62	-1.04	16	-0.25	-0.99	63.0	6.9	T
1859+03l	0.655	7.487	2440	8.7, ...	19	-0.91	-1.17	17	-0.49	-1.14	35.0	5.5	S_t
1900+05l	0.746	12.896	1014	...	6	-0.55	-1.07	44	-0.15	-0.77	28.0	4.7	S_t
1915+13l	0.194	7.202	4042	3.0, ...	11	-0.62	-1.01	48	-0.27	-1.06	68.0	9.7	S_t
1919+21l	1.337	1.348	1627	46.4, 7.5	0	-0.77	-0.77	0	-0.82	-0.82	45.0	3.9	cQ
1920+21l	1.077	8.189	1444	3.4, ...	14	-0.64	-1.12	81	-0.15	-0.90	44.0	5.7	T
1929+10l	0.226	1.156	2459	36.3, 11.5	0	-1.03	-1.03	0	-1.10	-1.10	90.0	42.2	T
1944+17l	0.440	0.020	1149	2.0, ...	91	-0.20	-1.64	87	-0.13	-1.10	19.0	6.7	T
1946+35l	0.717	7.052	1400	4.9, ...	13	-0.60	-1.20	49	-0.18	-1.04	34.0	5.5	S_t
2002+31l	2.111	74.570	490	5.2, ...	5	-0.55	-1.09	32	-0.08	-0.42	49.0	4.2	T
2016+28u	0.557	0.149	3843	60.3, 12.1	0	-0.98	-0.98	0	-0.96	-0.96	39.0	7.7	S_d
2016+28l	1610	3.8, ...	10	-0.64	-1.06	14	-0.16	-0.59
2020+28u	0.343	1.893	3000	56.1, 13.8	14	-0.72	-1.09	32	-0.69	-1.09	72.0	7.3	T
2020+28l	2699	12.4, 9.4	0	-0.84	-0.84	0	-0.78	-0.78
2044+15l	1.138	0.185	1055	7.8, ...	6	-0.53	-1.03	14	-0.27	-0.96	40.0	5.5	D
2053+36l	0.221	0.364	1615	...	5	-0.19	-0.71	89	-0.08	-0.54	34.0	0.0	S_t
2110+27l	1.202	2.622	1358	12.9, 12.7	6	-0.55	-1.07	32	-0.41	-1.15	76.0	5.3	S_d
2113+14u	0.440	0.290	1780	...	5	-0.76	-1.02	32	-0.38	-1.06	30.0	0.0	S_t
2303+30u	1.575	2.895	1470	23.5, 16.9	0	-0.91	-0.91	0	-0.83	-0.83	20.5	4.5	S_d
2303+30l	1009	12.1, 11.4	6	-0.73	-1.10	11	-0.49	-1.09

NOTES.—Col. (1) Pulsar name (suffix “l” observations at 1414 MHz and “u” at 430 MHz; cols. (2) and (3) P and \dot{P} ; col. (4) number of pulses observed; col. (5) S/N in average profile and the average S/N in single pulses, col. (6) pulse number where break in the total intensity correlation plot occurs; cols. (7) and (8) slope s_t^1 and slope s_t^2 (before and after the break); col. (9) pulse number where break occurs for the polarized power I_p ; cols. (10) and (11) slope $s_{I_p}^1$ and slope $s_{I_p}^2$ for I_p ; cols. (12)–(14) α , ρ , and pulsar type from Rankin 1993.

numbers n_I and n_{I_p} where the breaks in the slope occur for the total intensity profiles and the polarized power profiles, and the slopes s^1 and s^2 before and after the break.

In PSR 1929+10, the stabilization for the total profile, as well as a partial profile centered around the mainpulse, behaves in a similar manner. The stabilization behavior of a partial profile constructed around the region of the interpulse, however, has a very different behavior. This profile stabilizes rather slowly with a very flat slope, has a break in the slope between 16–32 periods, and stabilizes somewhat faster after this break. However, in view of the small signal-to-noise ratio (S/N) in the interpulse as opposed to the total pulse, this difference in the stabilization behavior seen between the main and the interpulse in PSR 1929+10, as well as other pulsars with interpsules, needs further study.

3. RATE OF STABILIZATION AND PULSAR PROPERTIES

We looked for correlations of the slopes of the $\log(1 - X_n)$ vs. $\log n$ plots with various pulsar parameters in order to understand the mechanisms which govern the stabilization rate. These correlations are reported in Table 2. No highly significant correlation with any intrinsic pulsar parameter is seen for the slopes s^1 and s^2 . However, the quantity $s_{I_{max}}$, which is the slope of the (straight part) of the variation $I_{max}(n) - \langle I_{max} \rangle$, the average peak intensity of subaverages of n periods, and the peak intensity of the global profile, shows a highly significant correlation with the quantities \dot{P} and $(P\dot{P})^{1/2}$ and is highly anticorrelated with the quantity $P/2\dot{P}$. This high degree of correlation is not reflected in the slope values s^1 and s^2 , as the subaverages are normalized in average intensity with respect to the global averaged profile while calculating the correlation coefficients. A moderately significant anticorrelation with $P/2\dot{P}$ is, however, observed for s^1_I , indicating that the older pulsars which spend a larger fraction of time in a null state (Ritchings 1976) converge slowly to a stable profile. This behavior can be seen rather dramatically in the case of the pulsar 1944+17, which spends a large fraction of time in a null state. The first slope for the polarized profile stabilization, s^1_p , is significantly correlated with the polar cap cone opening angle ρ (as determined by Rankin 1993), while s^2_p is signifi-

cantly anticorrelated with $(P\dot{P})^{1/2}$. Again, s^1 for the total intensity as well as the polarized flux is moderately correlated with α , the angle between the magnetic and rotation axis.

Oscillations of neutron stars could be one cause of irregular quasi-periodic variations in the pulse emission. It is unlikely, however, that this phenomenon could give rise to discrete variations like mode-changing and nulling observed in some pulsars. The investigator van Horn (1980) discusses quasi-periodic variations arising over several timescales ranging from a few milliseconds to a few years that could occur because of various types of oscillations of the neutron star crust. Non-radial g -mode oscillations are thermally induced by buoyancy perturbations in which gravity acts as the restoring force. The timescales of these oscillations are therefore dependent on the temperature of the neutron star crust and vary as the inverse of the square root of the surface temperature. All the pulsars considered here are old enough that the limiting temperature reached owing to interior vortex heating would be a more relevant temperature to consider than that obtained from cooling calculations. From the calculations of Shibazaki & Lamb (1989) the temperature variation with P and \dot{P} can be obtained, which then gives the oscillation timescale variation as

$$\tau_g \sim (P^2/\dot{P})^{1/4}$$

for an assumed constant moment of inertia for all neutron stars. From the negligible correlation seen of the slopes s with this parameter for the sample of pulsars considered here, it could be surmised that such thermally induced oscillations do not contribute to the irregular variations seen in pulsar emission. Alfvén modes considered by van Horn (1980) are oscillation modes where the magnetic field acts as the principle restoring force. The timescale for these oscillations varies inversely with the magnetic field strength. The slopes s , however, show a negligible correlation with $(P\dot{P})^{1/2}$ for the sample of pulsars considered here (although the intensity variations and their stability seem to be highly correlated with this quantity). This seems to indicate that neither Alfvén modes nor thermal oscillations play a role in the irregular pulse-to-pulse variations.

TABLE 2
CORRELATION OF STABILIZATION AND PHYSICAL PARAMETERS

Parameter	s^1_I	s^2_I	$s^1_I - s^2_I$	s^1_p	s^2_p	$s^1_p - s^2_p$	$s_{I_{max}}$	$s_{I_{whm}}$	$s_{\phi_{max}}$
P	-0.03 (0.85)	0.25 (0.15)	0.19 (0.26)	-0.12 (0.46)	-0.27 (0.11)	-0.07 (0.69)	0.27 (0.13)	-0.12 (0.50)	-0.13 (0.46)
\dot{P}	-0.11 (0.51)	-0.18 (0.30)	-0.07 (0.70)	-0.21 (0.21)	-0.36 (0.03)	-0.04 (0.80)	0.45 (0.009)	0.29 (0.09)	-0.04 (0.80)
$P/2P$	-0.37 (0.03)	0.23 (0.18)	0.36 (0.03)	-0.23 (0.16)	0.01 (0.95)	0.24 (0.15)	-0.50 (0.003)	-0.32 (0.06)	-0.23 (0.19)
$(P\dot{P})^{1/2}$	-0.05 (0.74)	-0.03 (0.87)	0.01 (0.95)	-0.24 (0.16)	-0.38 (0.02)	-0.03 (0.86)	0.64 (<0.001)	0.27 (0.13)	0.01 (0.95)
α	0.33 (0.05)	-0.13 (0.43)	-0.27 (0.11)	0.33 (0.05)	0.19 (0.28)	-0.20 (0.24)	0.39 (0.02)	0.21 (0.24)	-0.08 (0.66)
ρ	0.21 (0.20)	0.08 (0.64)	-0.06 (0.74)	0.42 (0.01)	0.22 (0.20)	-0.26 (0.13)	0.12 (0.51)	0.13 (0.46)	-0.15 (0.40)
$[P^2/\dot{P}]^{1/4}$	-0.22 (0.21)	0.19 (0.25)	-0.08 (0.65)	0.10 (0.58)	0.08 (0.65)	0.16 (0.37)	-0.01 (0.97)	0.28 (0.11)	<0.01 (0.99)
s^1_I	-0.28 (0.09)	-0.73 (<0.001)	0.80 (<0.001)	0.34 (0.04)	...	-0.02 (0.92)	0.24 (0.15)	0.07 (0.69)
s^2_I	-0.28 (0.09)	...	0.86 (<0.001)	-0.26 (0.13)	0.24 (0.16)

NOTES.—Col. (1) Pulsar parameter; cols. (2)–(10) correlation of the slopes listed in the top row with the parameters listed in the first column.

4. CONCLUSIONS

We conclude that the variations in the pulse profile from pulse to pulse are caused by physical processes which are remarkably stable. The stabilization rate seems to be related to the pulsar age, with the older pulsars converging more slowly to a stable profile. A correlation of the stabilization rate with the magnetic inclination angle is also seen, but whether this implies a perturbing process depending on the inclination angle is not clear without resolving the issue of how the inclination angle evolves with time. For most pulsars which do not show regular drifting or moding behavior, the location in phase of the pulse maximum is quite stable, so that the profile

variations from pulse to pulse seem to arise mainly from variations in the pulse intensity and pulse width. The stabilization rate for the polarized flux shows a strong correlation with the polar cone opening angle, whereas no correlation is seen for the total intensity.

The data used in this work were obtained in collaboration with Amy Carlow, Vera Izvekova, and Sveta Suleymanova. This research was supported by a grant from the National Science Foundation (AST 89-17722). Arecibo Observatory is operated by Cornell University under contract to the National Science Foundation.

REFERENCES

- Helfand, D. J., Manchester, R. N., & Taylor, J. H. 1975, *ApJ*, 198, 661 (HMT75)
Rankin, J. M. 1993, *ApJS*, 85, 145
Ritchings, R. T. 1976, *MNRAS*, 176, 249
Shibasaki, N., & Lamb, R. K. 1989, *ApJ*, 346, 808
van Horn, H. M. 1980, *ApJ*, 236, 899